

# Line-of-Sight Reddening Predictions: Zero Points, Accuracies, the Interstellar Medium, and the Stellar Populations of Elliptical Galaxies

David Burstein<sup>1</sup>

Received \_\_\_\_\_; accepted \_\_\_\_\_

arXiv:astro-ph/0306591v2 4 Aug 2003

---

<sup>1</sup>Department of Physics and Astronomy, Box 871504, Arizona State University, Tempe,  
AZ 85287-1504

## ABSTRACT

Revised  $(B-V)_0$ - $Mg_2$  data for 402 elliptical galaxies are presented which are used to test reddening predictions. These reddening predictions can also tell us both what the intrinsic errors are in this relationship among gE galaxy stellar populations, as well as details of nearby structure in the interstellar medium (ISM) of our Galaxy and of the intrinsic errors in reddening predictions. Using least-squares fits, the explicit  $1\sigma$  errors in the Burstein-Heiles (BH) and the Schlegel et al. (IR) predicted reddenings are calculated, as well as the  $1\sigma$  observational error in the  $(B-V)_0$ - $Mg_2$  for gE galaxies. It is found that, in directions with  $E(B-V) < 0.100$  mag (where most of these galaxies lie),  $1\sigma$  errors in the IR reddening predictions are 0.006 to 0.009 in  $E(B-V)$  mag, those for BH reddening prediction are 0.011 mag, and the  $1\sigma$  agreement between the two reddening predictions is 0.007 mag. IR predictions have an accuracy of 0.010-0.011 mag in directions with  $E(B-V) \geq 0.100$  mag, significantly better than those of the BH predictions (0.024-0.025). Both methods yield good evidence that gas-to-dust variations that vary by a factor of 3, both high and low, exist along many lines-of-sight in our Galaxy. Both methods also predict many directions with  $E(B-V) < 0.015$  mag, despite the difference in zero point that each has assumed. The  $\sim 0.02$  higher reddening zero point in  $E(B-V)$  previously determined by Schlegel et al. is confirmed, primarily at the Galactic poles. Independent evidence of reddening at the North Galactic pole is reviewed, with the conclusion that there still exists directions at the NGP that have  $E(B-V) \ll 0.01$ . Two lines of evidence suggest that IR reddenings are overpredicted in directions with high gas-to-dust ratios. As high gas-to-dust directions in the ISM also include the Galactic poles, this overprediction is the likely cause of the  $E(B-V) \sim 0.02$  mag larger IR reddening zero point relative to that of BH.

*Subject headings:* dust,extinction:Galaxy - Galaxy:ISM - galaxies:stellar content

## 1. Introduction

Maps of line-of-sight Galactic reddening (Burstein & Heiles 1978b) ushered in a new era in astronomy in which reddenings could be reliably predicted along arbitrary lines-of-sight. These maps supplanted the cosecant laws previously used to make such predictions (e.g., de Vaucouleurs, de Vaucouleurs, & Corwin 1976). The more recent method for predicting line-of-sight reddening (Schlegel, Finkbeiner, & Davis 1998) is also differentially accurate in its predictions, but assumes a zero point  $\sim 0.02$  mag higher in  $E(B-V)$  than does the Burstein & Heiles method. cursory examination of the reddening predictions listed for the Burstein & Heiles method and that of Schlegel et al. on the NASA Extragalactic Database (NED) website ([nedwww.ipac.caltech.edu](http://nedwww.ipac.caltech.edu)) shows that this difference in zero point produces a large difference in predicted B mag extinction ( $4.315 \times 0.02 = 0.086$  mag), and belies the actual good differential agreement between the two reddening predictions found in the present paper. Yet it is the 20-year experience of this author that very few astronomers take cognizance of this zero point issue. Schlegel et al. further claim that their method is significantly more differentially accurate than the Burstein & Heiles method (see the abstract and Sec. 5 of their paper).

§2 of the present paper presents the  $(B-V)_0$ - $Mg_2$  data for gE galaxies used for the reddening calibration tests in both this paper and in Schlegel, Finkbeiner, & Davis (1998). These data are a significant advance in calibrating *differential* reddening predictions over what was available from globular clusters and RR Lyrae stars in Burstein & Heiles (1978b). In §2, via a set of four coupled least-squares equations,  $1\sigma$  errors are explicitly derived in a least-squares sense for the Burstein & Heiles and the Schlegel et al. reddening predictions, as well as for the  $(B-V)_0$ - $Mg_2$  relation for gE galaxies. §3 discusses various related issues,

including: reddening at the North Galactic Pole (NGP); HI gas-to-dust variations in the interstellar medium (ISM); minimum line-of-sight reddenings; the stellar populations of galaxy groups; and systematic issues surrounding reddening predictions. The case is made in §4 that the zero point difference between the Burstein & Heiles reddening predictions and the Schlegel et al. reddening predictions is due to Schlegel et al. overpredicting reddenings in directions where gas-to-dust ratios are high. The major findings of this paper are summarized in §5.

## 2. Accuracy of the Reddening Predictions

### 2.1. The Reddening Calibration Data: Elliptical Galaxy Stellar Populations

The reddening prediction method developed by Burstein & Heiles (Burstein & Heiles 1978a,b, 1982, 1984, hereafter termed the “BH” method) uses the empirical fact that galaxy counts decrease with increasing extinction to monitor the varying HI column density-to-dust ratio that was discovered in Burstein & Heiles (1978b). The availability of maps of infrared emission in the sky in the 1980’s and 1990’s made it feasible to make new line-of-sight predictions of reddening using observations of emission by dust (Schlegel, Finkbeiner, & Davis 1998, hereafter termed the “IR” method), even if it is still not known what portion of the dust in the ISM produces the reddening that is seen in the optical (cf. Li & Greenberg 1997). One must assume a relation between extinction and  $E(B-V)$  to calculate extinction from these methods (e.g., a value of 4.315 is assumed by Schlegel et al. to convert  $E(B-V)$  to  $A_B$ ; BH used 4.0 for this conversion for reasons discussed in Burstein & Heiles (1978b)).

Neither set of reddening prediction methods directly measures the dust that is doing the line-of-sight reddening. Rather, each must assume a relationship between the measured quantity and the line-of-sight reddening. Both are therefore “differential” predictions of

line-of-sight *reddening* which need to be calibrated with external data. Burstein & Heiles (1978b) calibrated their method using globular cluster and RR Lyrae star reddenings. Since that time, the integrated stellar population properties of giant elliptical (gE) galaxies have been found to be so uniform that they can be used for accurate differential reddening measurements (Burstein et al. 1988; Faber et al. 1989).

At their request, this author provided Schlegel et al. with a set of  $Mg_2$  line strengths and (B-V) colors for gE galaxies taken from the 7 Samurai (Faber et al. 1989) database. The database this author provided Schlegel et al. differs from that published in Faber et al. (1989) in one important respect. The  $Mg_2$ -velocity-dispersion-(B-V) relationships (Bender, Burstein, & Faber 1993) among gE galaxies were used to put each subset of the 7 Samurai  $Mg_2$  data on a consistent system.<sup>2</sup> The corrected  $Mg_2$  measures for each data subset are then added back together with the rest of the 7 Samurai  $Mg_2$  data, and new average values of  $Mg_2$  for affected galaxies are calculated. Since this effectively produces a new set of data, the full set of these  $Mg_2$  data are being made available with this paper (cf., Hudson 1999, where a portion of these data were also presented).

Table 1 gives the first 10 lines of the reddening-related data used in this paper for elliptical galaxies; the full list for 402 gE galaxies is available via anonymous ftp from

---

<sup>2</sup>Published  $Mg_2$  values (cf. Davies et al. 1987) for several subsets of the 7 Samurai data have been modified: -0.012 mag added to LCO H1 data, 0.014 mag to LCO H2, +0.011 mag to LCO 2D, and +0.020 mag to AAT1. (The LCO H1, LCO H2, LCO 2D and AAT1 subsets refer to the telescopes and observing runs used by members of the 7 Samurai to obtain spectroscopic data for these galaxies. The LCO data was taken at the Las Campanas Observatory, and the AAT data taken at the Anglo-Australian Telescope. The labels H1, H2, and 2D refer to the different spectrographic configurations used for the LCO spectra; see Davies et al. for details.)

samuri.la.asu.edu/pub/burstein/bvmg2 (bvmg2\_Table\_1\_burstein03.lst). 13 gE galaxies do not have direct BH or IR reddenings (see the notes to Table 1 for details). A further 11 gE galaxies in the region  $230^\circ < l < 310^\circ$ ,  $-20^\circ < b < 20^\circ$  were found in Lynden-Bell et al. (1988) and Burstein et al. (1987) to have HI-only BH reddening predictions that are a factor of two too high (These galaxies are given in the notes to Table 1 and are noted in the ASCII version of this table by an asterisk in their names.) Burstein et al. predicted reddenings for these 11 galaxies use the  $(B-V)_0$ -Mg<sub>2</sub> relation, so 7 Samurai reddenings cannot be used for these galaxies. Rather, the values of  $E(B-V)$  for these 11 galaxies predicted from the BH method have been uniformly halved to go with the higher gas-to-dust ratio found by the 7 Samurai. (The reddenings for these 11 galaxies are separately discussed below.) It may be a bit confusing, but it should be noted that an additional 11 galaxies within a smaller region (see notes to Table 1) did *not* need to have their reddenings so-corrected in the 7 Samurai database. These other 11 galaxies include several which are as reddened as the galaxies that *do* require gas-to-dust corrections. Evidently, this southern region has a mixture of regions of high gas-to-dust ratios and regions of normal gas-to-dust ratios.

Twenty-four (24) galaxies are thus objectively excluded from the least-squares error-determination analysis of this paper. This yields 378 gE galaxies with direct BH *and* direct IR reddening predictions. To make sure that the reddenings used for the IR method are those in the public domain on the NASA Extragalactic Database (NED) website, the NED group kindly provided this author with the IR reddenings for the galaxies in this sample.<sup>3</sup>

---

<sup>3</sup>The NASA/IPAC Extragalactic Database (NED) is operated by the Jet Propulsion Laboratory, California Institute of Technology, under contract with the National Aeronautics and Space Administration.

## 2.2. Observational and Intrinsic Accuracies of Reddening Methods

The 378 gE galaxies are divided into three samples: those with reddenings  $E(B-V) \leq 0.100$  averaged from both methods (the “low” reddening sample); those with  $E(B-V) > 0.100$  (the “high” reddening sample), and the full sample taken as a whole. (The rationale for separating galaxies into low/high reddening directions is given below). No separation is made at the dividing line for the BH method (declination =  $-23.5^\circ$ ), south of which the BH predictions change their methodology from use of both galaxy counts and HI column densities to use of only HI column densities. Schlegel, Finkbeiner, & Davis (1998) did not find a difference in these two regions, save the  $l = 230 - 310^\circ$  region identified above. Note that only HI values are also used at high Galactic latitudes ( $b > |65^\circ|$ ) in the BH method, as galaxy counts become correlated in real space above those latitudes; (cf., discussion in Burstein & Heiles 1978b).

IR and BH reddening predictions first must be placed on the same zero point scale. This can be done in two ways, using all 378 galaxies: a) Zeroing IR predictions to BH predictions yields a *median* offset of 0.016 mag in  $E(B-V)$ , which is then subtracted from the IR predictions; b) Zeroing BH predictions to IR predictions requires adding a median offset of 0.019 mag in  $E(B-V)$  to the BH predictions. Both zero point offsets are consistent with the  $E(B-V) = 0.02$  zero point difference between IR and BH methods found by Schlegel et al. (estimated only in directions with  $b > |45^\circ|$ ; i.e. the Galactic poles.)

The slight difference (0.003 mag) in zero point difference calculated these two ways is because negative BH reddenings are routinely given for the BH method, owing to the existence of HI gas with no measured reddening. BH acknowledged from the outset that their zero point could be in error by 0.01 mag in  $E(B-V)$  (cf. Burstein & Heiles 1982). While negative values of reddening are explicitly calculated in the BH method, these predicted reddenings are set to zero if they are used as reddenings (cf. Burstein & Heiles

1984). Thus, if a different reddening zero point was established, adjustment of the BH reddening predictions would then only require addition of the new zero point (as used here). In contrast, the IR method defines its zero point as formally 0.000. Hence, adjusting BH zero point to IR zero point results in some negative BH reddenings becoming positive, but adjusting IR zero point to BH zero point results in some IR reddenings becoming negative (and are therefore set to 0.000 for reddening calculations). There are 351/27 low/high reddening galaxies when the 0.016 mag zero point difference is subtracted from the IR method, and 344/34 low/high reddening galaxies when the 0.019 mag zero point difference is added to the BH method. For each zero point used, averages of the two reddening predictions (i.e, BH+IR-0.016 and IR+BH+0.019) are also calculated.

The  $(B-V)_0$ - $Mg_2$  relationship for gE galaxies are fit via two equations:  $(B-V)_0 = 1.12 Mg_2 + \text{constant}$  and  $(B-V)_0 = 0.942 Mg_2 + \text{constant}$ . The 1.12 slope comes from Bender, Burstein, & Faber (1993), who show that the  $(B-V)_0$ - $Mg_2$  relationship extends over a much wider range of color than is given for just the 7 Samurai galaxies. The 0.942 slope is derived from only the gE data used here. Use of either slope, with the appropriate choice of constant, yields very similar results for the gE dataset. Constants for these equations are chosen to yield zero *median* values of residuals for the 378 galaxies sample: for the 1.12 slope, they are 0.600, 0.601, 0.601, 0.618, 0.617, and 0.618 respectively for the BH, IR and Average values (respectively), with the BH+0.019 & IR values listed first, and the BH & IR-0.016 values listed second. Analogously, they are 0.654, 0.654, 0.655, 0.672, 0.669, 0.670 for the 0.942 slope.

It is assumed that all deviations from the  $(B-V)_0$ - $Mg_2$  relation are due to a combination of random observational and cosmic errors for the reddening predictions and in the  $(B-V)_0$ - $Mg_2$  relationship for gE galaxies. Handling the data in the manner described above gives 12 ways of looking at these data: two different zero points, two different slopes of the

$Mg_2$ -(B-V)<sub>0</sub> equation, and three subsamples: low, high and ‘all’.

For each of these 12 ways, there are four observationally-independent  $1\sigma$  errors we can calculate i) the error of BH reddening predictions on the (B-V)<sub>0</sub>- $Mg_2$  relationship ( $\sigma(\text{BH} : \text{BV})$ ); ii) the error of the IR reddening predictions on the (B-V)<sub>0</sub>- $Mg_2$  relationship ( $\sigma(\text{IR} : \text{BV})$ ); iii) the error of the average (BH+IR) reddening prediction on (B-V)<sub>0</sub>- $Mg_2$  relationship ( $\sigma(\text{Ave} : \text{BV})$ ); iv) and the  $1\sigma$  error for the the agreement in reddening predictions of BH to IR ( $\sigma(\text{BH} : \text{IR})$ ). (No individual weighting is given each galaxy, as the 7 Samurai cited only average errors for these data.) In turn, each observable error is itself the quadratic sum of the intrinsic errors for each data set:  $\sigma(\text{BH})$ ,  $\sigma(\text{IR})$ ,  $\sigma(\text{Ave})$ , and  $\sigma(\text{BV} + Mg_2)$ . This gives us four equations in four unknowns which relate the observable errors to these intrinsic errors:

$$\sigma(\text{BH} : \text{BV})^2 = \sigma(\text{BH})^2 + \sigma(\text{BV} + Mg_2)^2,$$

$$\sigma(\text{IR} : \text{BV})^2 = \sigma(\text{IR})^2 + \sigma(\text{BV} + Mg_2)^2,$$

$$\sigma(\text{Ave} : \text{BV})^2 = \sigma(\text{Ave})^2 + \sigma(\text{BV} + Mg_2)^2,$$

and

$$\sigma(\text{BH} : \text{IR})^2 = \sigma(\text{BH})^2 + \sigma(\text{IR})^2.$$

Intrinsic errors are determined via a least-squares analysis. Table 2 gives the results of this least-squares analysis, two lines for each of the 12 ways of looking at these data (see the table notes for an explanation to Table 2). Figures 1, 2 and 3 show results from using

the 1.12 slope for the  $(B-V)_0$ - $Mg_2$  relation, as results from the 0.942 slope are virtually indistinguishable from these data (cf. Table 2). Figures 1a-f are histograms of residuals from the  $(B-V)_0$ - $Mg_2$  relation for the 378 gE galaxies, divided into low and high reddening subsets. Figures 1a-c are the residuals from the  $(B-V)_0$ - $Mg_2$  relation for gE galaxies using (a) the IR-0.016 values, (b) the original BH values, and (c) the average of these two reddening predictions. Figures 1d-f are analogous to Figures 1a-c, but calculated using (d) the original IR values, (e) the BH+0.019 values, and (f) the average from these values.

Figures 2a-f (parallel to Figures 1) give the scatter in these reddening predictions versus the average value of reddening for both samples of the data for each kinds of zero points these gE galaxies, now including the 11 high gas-to-dust galaxies in the  $230^\circ < l < 310^\circ$ ,  $-20^\circ < b < 20^\circ$  region that were not included in the least-squares analysis. Different symbols are used to denote these 11 galaxies, as well as the 8 galaxies in the Perseus cluster (the most-reddened galaxies in this sample that are all in one direction), as these galaxies are discussed separately below. Figures 3a,b show the histograms of the scatter in the BH and the IR reddening predictions for these gE galaxies, again with the two subsets of highly-reddened samples distinguished; Figure 3a for BH vs. IR-0.016, Figure 3b for BH+0.019 vs. IR.

It is evident upon inspection that the distribution of reddening residuals for the low reddening galaxies (Figures 1) are reasonably Gaussian, consistent with the initial assumption that random errors dominate these data, and ex post facto justification of the least-squares analysis performed here. It is also evident that the reddening residuals for the high-reddened sample do not define a reasonable Gaussian sample (making their least-squares analysis a bit suspect), suggesting that other issues might be at play when line-of-sight reddening is high.

The  $1\sigma$  least-squares error for the relationship of  $Mg_2$  on  $(B-V)_0$  is 0.027 mag for the

low reddening galaxies (lines 2, 5, 8, and 11 of Table 2)), as well as for the whole 378 galaxy sample (lines 1, 4, 7, and 10 of Table 2). Consistency of errors determined for the  $M_{g_2}-(B-V)_0$  relation for all low reddening subsets of these data further justifies the Gaussian assumption for the least-squares fits to these data.

Galaxies with high Galactic reddening are generally situated at low Galactic latitudes and/or in regions with irregular stellar foregrounds. This observer can attest to the difficulties in obtaining reliable (B-V) colors for such galaxies. Hence, a larger scatter in the  $M_{g_2}-(B-V)_0$  relation for high reddening galaxies was expected (and is the reason for dividing the data set into low and high reddening areas).

The  $1\sigma$  agreement in reddening between the BH and IR methods for 378 gE galaxies is either 0.0144 mag (IR-0.016:BH) or 0.0158 mag (BH+0.019:IR), for an average  $1\sigma$  scatter between these reddening predictions of 0.0151 mag. The  $1\sigma$  errors of reddening predictions in low reddening directions are 0.006-0.009 mag for the IR method, and 0.011 mag for the BH method, with BH and IR predictions methods agreeing to an accuracy of 0.007 mag in these directions. In the high reddening areas (but excluding the “southern” region with high gas-to-dust ratios), errors remain 0.011 mag for the IR method but increase to 0.024-0.025 mag for the BH method. Line 2 of Table 2 also shows some evidence of skewness in the IR predictions for high reddening areas, yielding a mean of 0.005 mag when the median is chosen to be zero; the BH values for high reddening areas show negligible skewness.

Taking the 378 galaxy sample as a whole, the IR values yield more accurate reddenings based on these elliptical galaxy data than do the BH predictions, 0.007-0.009 mag to 0.013 mag. So, while Schlegel et al. were correct in stating that the IR method is more accurate than the BH method, in reality it is a difference in reddening predictions over most of the sky that is measured in millimag (i.e., a difference generally not detected by users of either method).

### 3. ISM Issues and gE Stellar Populations

#### 3.1. Polar reddening

Burstein & Heiles (1982) give a major review of reddening at the Galactic poles, in which they determined the direction of lowest reddening (found at the North Galactic pole) from the average reddening of BAF stars determined by both the  $uvby\beta$  method and the average interstellar polarization of those stars. In turn, this direction of lowest reddening (consistent with zero reddening as measured by these indicators) was used to determine the BH zero point. In contrast, Schlegel, Finkbeiner, & Davis (1998) determine the average reddening at the NGP by directly measuring infrared emission, and assuming a one-to-one relation between IR dust emission (modulated by dust temperature) and reddening. Hence, in both methods, the zero points assumed and the average value of reddening at the Galactic poles are linked.

Since Burstein & Heiles (1982), various authors have tried to show that the reddening at the NGP is more than obtained in that review, Schlegel et al. included. Schlegel et al. give two arguments in support of their finding non-zero reddening at the NGP: First, they cite the study of Teerikorpi (1990), which claims that low reddening at the NGP is an artifact due to stellar samples which select against more reddened stars (a type of selection effect previously pointed out by Burstein & Heiles (1978a) in connection with galaxy selection issues; see §3.6). Second, Schlegel et al. suggest that dust ablation that could occur at the NGP would not eliminate “the small grains that dominate the UV and optical extinction.”

The Teerikorpi analysis leaves several issues unresolved, namely:

1. The fact that both BH and IR methods predict some measurable reddening ( $E(B-V) \sim 0.01-0.03$  mag) within  $15^\circ$  of the NGP, and that this reddening is likely at a

distance of 150-250 pc from us (cf. Burstein & Heiles 1978b) is ignored. No check was made if the reddening shown in Figure 2 of Teerikorpi (1990) is correlated in position on the sky or if directions with zero reddening are also correlated on the sky.

2. A claim is made that predicted  $E(b-y)$  is higher for more luminous, bluer (and more distant) AF stars. However, this effect is seen for all of the distance bins in Figs. 4 and 5 of that paper, including that for the nearest stars (for which no selection bias is claimed in Teerikorpi’s analysis). This suggests more a calibration error in the reddening predictions for the bluest stars in his sample, rather than the kind of reddening-dependent selection effect proposed by Teerikorpi. This calibration error would also explain the higher reddening that Teerikorpi obtains from the  $uvby\beta$  data than was obtained by Burstein & Heiles (1982).

3. It is stated that there is a general reddening of  $E(B-V) = 0.04$  mag over the whole NGP. Yet, the average  $E(B-V)$  determined by the IR method is 0.015 mag, averaged over  $10^\circ$  around the NGP (Schlegel, Finkbeiner, & Davis 1998), and that of BH is consistent with this picture, but at a bit less reddening.

Berdyugin & Teerikorpi (cf. 2002) have also recently published new polarization measurements of stars at the NGP. Their measurements indicate large regions around the NGP where no polarization of starlight is measured, consistent with the directions absent of stellar polarizations found by Appenzeller (1975) and Markannen (1979) (the data used by BH in 1982 to help establish their zero point). The new stellar polarization measures of Berdyugin & Teerikorpi (2002) actually strengthen the result that the NGP contains regions with line-of-sight  $E(B-V) \ll 0.01$  mag.

It is relevant here that Burstein & Heiles (1978b) and Burstein & Heiles (1982) point out that high gas-to-dust ratios exist preferentially as halos around nearby OB associations at low latitudes. (Those high gas-to-dust ratios *cannot be due* to either molecular clouds, or

missing HI flux in the HI maps used by Burstein & Heiles (a suggestion made by Boulanger, et al. (1996)), as both effects would lower the gas-to-dust ratio, not raise it.)

Not all the dust that produces emission produces reddening in the UV and optical (cf. Li & Greenberg 1997); a point also made by Schlegel et al. However, the halos of the OB associations tell us that the outflows from these associations can diminish the reddening from the dust while not diminishing the HI gas. It is known that our solar system is passing through an HI superbubble of the type originally identified by Heiles (1979) (cf. discussion in Strittmatter, et al. 1984). Hence, our Sun is now within a region that is analogous to the outflow halos of the OB associations, so by analogy, high gas-to-dust ratios are likely at high Galactic latitudes. Greenberg & Li (1995) suggest that high gas-to-dust regions could be due to the outflows whittling down the ice mantles on the dust such that more small grains are produced relative to larger grains, reducing the UV and optical extinction.

In summary, the NGP has a patchy distribution of low amounts of reddenings, including directions where  $E(B-V) \ll 0.01$  mag with no measurable polarization of the stars. Yet, in all directions in the NGP, there are quite measurable amounts of HI column density. The conclusion arrived at by BH in 1982 still stands, namely that the NGP is a region where the gas-to-dust ratio is high.

### 3.2. Gas-to-dust variations

The dust-to-gas map (Figure 11) in Schlegel, Finkbeiner, & Davis (1998) shows gas-to-dust ratio variations of a factor of 3, both high and low. This is consistent with what was found in Burstein & Heiles (1978b). Schlegel et al. also find there are significant gas-to-dust ratio variations in directions where they also find low reddenings (their Table 5). Among the 9 of the 18 directions with HI measures, the HI-to-dust emission ratio varies by

nearly a factor of three. Hence, gas-to-dust variations along lines-of-sight in our Galaxy are real and pervasive.

Partly to study gas-to-dust variations, Boulanger, et al. (1996) combined their Leiden/Dwingeloo HI survey with COBE IR data, but restricted their analysis to regions with HI column densities of less than  $5 \times 10^{20} \text{ cm}^{-2}$  (224 BH units of HI column density). This limits their investigation to northern Galactic latitudes  $> 65^\circ$ . Boulanger, et al. (1996) find no variation in gas-to-dust ratio in their analysis. Yet, it is precisely at high Galactic latitudes that the BH method assumes a constant HI gas-to-dust ratio to predict accurate reddenings. Hence, there is no disagreement between the BH conclusions and those of Boulanger, et al. about the relative constancy of gas-to-dust ratios at high northern Galactic latitudes. And, conversely, the Boulanger et al. analysis says nothing about gas-to-dust ratio variations in the Galaxy at lower Galactic latitudes

It is evident that something has to happen to the dust to make its reddening characteristics get lower relative to the HI gas when it is found in regions of outflow around OB associations. Given that the most likely origin of Heiles-type HI superbubbles are interactions with outflow winds of OB stars and supernovae, it is likely that the dust emission seen at high galactic latitudes has the same reddening-reduced characteristics as that around the OB associations. This then would explain the observations of high gas-to-dust ratios for high latitude dust.

### **3.3. Zero Points of the Reddening Predictions vs. Minimum Reddening Lines-of-Sight**

The BH method predicts large sections at high Galactic latitudes where reddening is predicted to be zero. Given the estimated error in BH zero point (see above), this

really means lines-of-sight where  $E(B-V) < 0.01$  mag. Eighteen (18) directions in Table 5 of Schlegel et al. yield line-of-sight  $E(B-V)$  estimates of 0.003 to 0.015 mag; most have  $E(B-V) \ll 0.01$  mag. Among the 402 gE there are 62 with low IR-predicted  $E(B-V)$ , including five with  $E(B-V) \leq 0.008$  mag.

The fact that the zero point of the IR method is 0.02 mag higher than that of the BH method does not prevent the IR method from predicting reddenings with  $E(B-V) \leq 0.015$  mag in many directions on the sky. In other words, the zero point difference between the IR and BH methods is *not* due to the IR method predicting at least 0.02 mag of  $E(B-V)$  reddening all over the sky. Rather, this zero point difference arises from the different assumptions made by both BH and IR on how their reddening indicators correlate with reddening. The specific issue of the IR zero point is considered in detail below (§4). Here we note many papers have pointed out that if line-of-sight reddening is always non-zero, a wide range of astrophysical issues are affected. Not the least of these are the ages of Galactic globular clusters (VandenBerg, Bolte, & Stetson 1990), as for every 0.01 mag that the  $E(B-V)$  values are wrong, age errors of 1-2 Gyr are made.

### 3.4. Significant Differences and Two Specific Directions

In the difference map of BH and IR reddening predictions (Figure 12 in Schlegel et al.) are areas, mostly at low Galactic latitudes, where the two sets of predictions vary significantly. However, it is not sufficient to simply calculate the differences in reddening predictions for the BH and IR methods, as illustrated by the development of the HI-to-reddening relations in the BH papers. One needs to have independent reddening estimates to identify which, if either method, is in error.

Figure 5 plots the difference in BH and IR predictions versus the residuals from the

$(B-V)_0$ - $Mg_2$  relation for the gE galaxies. Lines are drawn at the  $\pm 0.0453$  mag level (i.e.,  $3 \times 0.0151$  mag) to identify those galaxies for which the BH and IR reddening predictions differ significantly. Nine galaxies, mostly in high-reddening directions, have predicted reddenings that differ by more than 0.043 mag (see Table 3). Interestingly, for all but one of these 9 galaxies, the IR reddening is significantly higher than the BH reddening. Inspection of Table 3 shows that four galaxies have IR reddening predictions better than BH predictions, four galaxies have BH predictions better than IR predictions, and for one galaxy both predicted residuals are within  $3\sigma$ , but of opposite sign.

Two specific regions in the sky were initially singled-out for special examination: the Perseus galaxies and the 11 galaxies in the “southern region” specified above. Figure 4 shows the predictions of the BH and IR methods differ systematically for the Perseus galaxies (cf. Table 3) which all lie in the same direction of the sky. Examination of BH and IR predictions for the  $(B-V)_0$ - $Mg_2$  relation for these eight galaxies reveals that the IR prediction has smaller errors for six of the eight galaxies. However, for three of the galaxies both IR and BH errors are large. The Perseus galaxies are among the lowest-latitude, most heavily-reddened galaxies in the 7 Samurai sample. It is worth emphasizing again the observational difficulties of obtaining accurate B and V magnitudes for galaxies in highly-reddened, crowded stellar fields.

The 11 highly-reddened galaxies in the region  $230^\circ > l > 310^\circ$ ,  $-20^\circ < b < 20^\circ$  had their BH reddening predictions halved for this paper. In contrast to the “note-added-in-proof” in the Schlegel, Finkbeiner, & Davis (1998) paper, the adjusted BH predictions are in generally good agreement with gE galaxy colors (cf. Table 3). It is also noted that only 3 of these galaxies are in the much smaller region  $230^\circ > l > 240^\circ$ ,  $-15^\circ < b < -10^\circ$  pointed out in the Schlegel, Finkbeiner, & Davis (1998) paper as having HI observational problems. The differences in predicted reddenings between BH and IR methods for these

11 gE galaxies will be discussed in detail in §4.

### 3.5. The stellar populations of gE galaxies

(B-V)<sub>0</sub>-Mg<sub>2</sub> relation errors include three sources: observational errors for (B-V) and Mg<sub>2</sub>; cosmic scatter among these stellar populations; and cosmic scatter in the gradients of these stellar populations *within* gE. At minimum, one has to assume an average observational error in Mg<sub>2</sub> of 0.01 mag (cf. Davies et al. 1988), and an observational error of 0.02 mag in (B-V) (as the original estimate of 0.03 mag in Burstein et al. 1987 cannot be correct). One is therefore left with a residual cosmic scatter of only 0.011 mag. This small cosmic scatter shows us that the stellar populations of gE, at least as measured through the (B-V) color and the Mg<sub>2</sub> index, are remarkably uniform both in overall terms, as well as in their internal gradients (see Trager, et al. (2000) for reasons why this might be the case). Couple this with the strong relation of stellar population with kinematics found in Bender, Burstein, & Faber (1993), and one has some very severe constraints on how the family of elliptical galaxies has to be formed.

Of the 344/351 galaxies in low reddening directions, six galaxies have good agreement in BH and IR reddening predictions, but have  $\geq 0.07$  mag deviations in their (B-V)<sub>0</sub> colors, having them both too blue (2 galaxies) and too red (4 galaxies) for their Mg<sub>2</sub> measurements (see Table 3). The two galaxies which are too blue for their Mg<sub>2</sub> values have BH and IR reddening predictions that are too small to compensate for the blueness of their (B-V)<sub>0</sub> colors. Five of these galaxies have close, early-type galaxy companions (cf., Tully 1988; Faber et al. 1989), while the sixth galaxy is in the Coma cluster (for which a close companion is hard to determine). It would be worthwhile to study the stellar populations in these 6 galaxies in more depth.

### 3.6. Why the IR method should be more accurate than the BH Method

In Burstein & Heiles (1978a) was concerned with the result of Sandage (1973, 1975), who obtained a *csc-law* slope that was smaller (0.03 mag) in  $E(B-V)$  than that obtained by others at that time (0.05 mag). What Burstein & Heiles (1978a) found is the  $gE$  at low Galactic latitudes used by Sandage to calibrate his *csc-law* (ironically, in the Perseus cluster) lie preferentially in areas of low reddening compared to other lines-of-sight in the same region. In choosing galaxies (or stars) for study, one chooses brighter galaxies (stars) which lie preferentially in directions of lower Galactic reddening.

Now couple this selection effect with the fact that the distribution of dust is very patchy on all size scales on which it has been measured (cf. Schlegel, Finkbeiner, & Davis 1998), and the levels of patchiness increase and the size scales of the patchiness decrease as reddening increases. As a result, the predictive power of any line-of-sight reddening prediction of finite pixel size will deteriorate in accuracy as the line-of-sight reddening increases, and/or with larger pixel size.

On average, galaxies (or stars) chosen on the basis of their brightness will be chosen in regions that have less reddening than the average around them. This effect is minimal for low-reddening directions, where variation in reddening is mostly comparable to or larger than either the BH or the IR pixels, but becomes important for highly-reddened regions, where patchy reddening exists on small angular size-scales. Hence, there will be a tendency for both the BH and the IR methods to overestimate the reddenings of highly-reddened galaxies (i.e., produce galaxies with colors too blue), with the onset of these systematic effects occurring at lower reddenings for the larger BH prediction pixel than for the smaller IR pixel. This is likely the primary reason why the IR predictions are more accurate than the BH predictions in highly-reddened directions, and slightly more accurate in low-reddening directions.

Inspection of Figures 2 shows that for  $E(B-V)(Ave)$  above 0.15 mag, there is a tendency for the BH method to, indeed, overpredict the reddenings of the galaxies (makes the galaxies too blue). Inspection of Figure 6 in Schlegel, Finkbeiner, & Davis (1998) shows that for reddenings larger than  $E(B-V) = 0.20$  mag, the IR-predicted values also systematically overestimate the observed reddenings. This is yet another reason for one to be careful if one wishes to extend either of these reddening prediction methods to high-reddening directions.

Many of the 7 Samurai galaxies with high reddenings are south of  $\delta = -23.5^\circ$ , and only have HI predictions from the BH method. The fact that there is no zero point shift, even for the 11 “southern” gE whose HI-predicted BH reddenings have been halved (see §4) indicates good consistency of HI measures, north and south.

### 3.7. Completeness Issues

BH: Areas in the south Galactic polar cap are missing BH predictions, as well as some directions elsewhere in the sky. The region  $230^\circ > l > 310^\circ$ ,  $-20^\circ < b < 20^\circ$  needs special attention (see above). The reddening for M31 is that of M32 in the BH method, as the HI of M31 interferes with the measurement of HI in our Galaxy.

IR: There might be an overestimate of its zero point and higher scatter in their predictions related to high gas-to-dust ratios (§4). No reddening prediction is made for M32, as the contribution of background M31 flux is uncertain (the opposite problem for this pair of galaxies than that faced by the BH method). The 5% of the sky not covered by the IRAS survey will have lower spatial resolution of the COBE/IR prediction than the rest of the sky.

#### 4. The IR:BH Zero Point Difference: A Matter of High Gas-to-Dust Ratios?

Examination of the Schlegel et al. paper finds that the dust:HI emission ratio image (their Figure 11) looks very similar to the IR:BH difference image (their Figure 12). Superimposing these two images confirms this impression: even very fine structure in the HI:dust emission map is the same as that in the IR:BH map. However, if we compare Figure 11 of Schlegel et al. to the relevant figures in Heiles (1976) (cf., discussion in Burstein & Heiles 1978b), then a curious difference emerges. The regions that are low gas-to-dust ratio in the Heiles maps correspond to regions where there is active star formation, and the regions of high gas-to-dust ratio surround these regions. As discussed in the BH paper, this makes sense if the high gas-to-dust ratio gas is due to the outflows from the star-forming regions. In contrast, in Figure 11 of Schlegel et al. the opposite occurs, as areas of *higher* gas-to-dust ratio tend to appear on that map *inside* regions of *lower* gas-to-dust ratios. This discrepancy could be solved if Figure 11 of Schlegel et al. is really a map of gas-to-dust ratios, rather than what they advertise it to be. For now, however, this discrepancy stands.

There are two regions sampled by the gE galaxies where it is known a priori that the HI/dust ratio is high: around the North Galactic Pole and the 11 “southern” region  $230^\circ > l > 310^\circ$ ,  $-20^\circ < b < 20^\circ$ ). Borrowing on the correlation seen for Figures 11 and 12 of Schlegel et al., their Figure 12 shows this “southern” region has the signature of patchy high gas-to-dust ratios. These 11 galaxies are listed in Table 3 (all 11 have an asterisk in their names).

Given that this is the only region for which there are both highly-reddened galaxies, and high gas-to-dust ratios, it is of interest to separately calculate the IR and BH reddening prediction errors for these particular 11 galaxies (these were not included in the error determination previously done). The value  $\sigma(\text{IR} : \text{BV})$  is 0.0337 for the IR reddening predictions for these 11 galaxies, significantly higher than 0.0212 found for  $\sigma(\text{BH} : \text{BV})$ .

While 0.0337 for  $\sigma(\text{IR} : \text{BV})$  is not out of line for IR values for high-reddened galaxies (cf. Table 2), the value of 0.0212 for  $\sigma(\text{BH} : \text{BV})$  is significantly smaller than its values for high-reddened galaxies. Moreover, further inspection of Table 2 shows that the values of  $\sigma(\text{IR} : \text{BV})$  are always smaller than those of  $\sigma(\text{BH} : \text{BV})$ . It is in this one region of space, where we have galaxies with high reddening *and* high gas-to-dust ratios, that the value of  $\sigma(\text{IR} : \text{BV})$  is much larger than that of  $\sigma(\text{BH} : \text{BV})$ .

Equally important, the IR method has a zero point overprediction of 0.0165 mag in E(B-V) for these 11 galaxies, relative to the BH predictions (even after the average zero point difference between the two methods is eliminated). For these 11 galaxies the average zero point difference between IR and BH predictions is 0.033 mag in E(B-V), not 0.016 mag as found for the 378 gE sample (from which these 11 galaxies were excluded).

As reviewed in §3.1, there is good reason to think that the Galactic poles are dominated by regions of high gas-to-dust ratios, similar to that found around OB associations, as we may be passing through the remnants of an old, Heiles-like superbubble in the ISM. As Schlegel et al. restricted their determination of the IR:BH zero point difference to directions with  $|b| > 45^\circ$ , it is precisely around the Galactic poles that their zero point difference of E(B-V) = 0.02 mag was calculated. Moreover, half of the 378 gE sample lie above Galactic latitudes of  $45^\circ$  (which is less than 1/2 of the sky).

The current evidence indicates that in regions of higher reddening, the IR minus BH zero point difference doubles to 0.033 mag. *Hence, if the IR method overpredicts E(B-V) in directions of high gas-to-dust ratios, with the size of the overprediction increasing as the degree of reddening increases, this would fully explain the zero point difference seen between the two methods.*

Appealing to Table 5 of Schlegel et al. for further information is of no avail, as IR (and BH) predicted E(B-V) in the 9 directions in that table having HI measures are  $< 0.015$

mag. The mutual agreement between the BH and IR methods, 0.007 mag in regions of low reddening, is comparable to this range of  $E(B-V)$ , making it fruitless to try to use these 9 directions to see if a relation exists between gas-to-dust ratio and the IR vs. BH zero point. One needs more highly-reddened, high gas-to-dust directions to make this test, the only such region in the present dataset is the southern hemisphere region discussed here.

The principal difference between BH and IR methods is that the BH method explicitly accounts for dust-to-gas ratio differences at low Galactic latitudes, while the IR method does not. As discussed in the previous section, there is reason to believe that variations in gas-to-dust ratio along different lines-of-sight in the Galaxy (which the IR method *does* confirm exist) are due to the modification of the dust grains in outflows from OB stars and supernova (cf. Greenberg & Li 1995).

Thus, there are two lines of evidence that strongly suggest the IR method overestimates reddenings in directions with high gas-to-dust ratios: First, the IR method has a 0.016 mag in  $E(B-V)$  higher zero point than the BH method as primarily determined in regions of low reddening, with half the sample near the Galactic poles. Second, the IR predictions overestimate reddenings at twice this level relative to those from the BH method for highly-reddened galaxies in the one low latitude, high gas-to-dust region that is sampled by the 7 Samurai data set. A third, related issue is the close correlation of fine-leveled structure in the IR:HI and IR:BH maps in Schlegel, Finkbeiner, & Davis (1998).

It is worth reflecting on the fact that to further test the IR predictions in regions of high gas-to-dust ratio and of moderately high reddenings, one is restricted to directions at relatively low latitudes. Yet, very few galaxy surveys include galaxies at low latitudes in their samples (unless one is probing the Zone of Avoidance itself). That there are any gE galaxies at low Galactic latitudes in the 7 Samurai sample is an accident of galaxy selection. Rather, most investigations of galaxies avoid highly-reddened regions more because they

lie in crowded stellar regions than they lie in highly-reddened directions (cf. the relatively high Galactic latitude limits of the Sloan Digital Sky Survey). Also due to the accident of their selection (from the ESO survey plates), most of the highly-reddened galaxies in the 7 Samurai survey lie below declination  $-23.5^\circ$ , the nominal northern galaxy count survey limit. Unless a concerted effort is made to study gE galaxies at low northern hemisphere latitudes (with their concomitant observational problems) in directions where there is known high gas-to-dust ratios, further probing of the issue of high gas-to-dust dependency of the IR method (and the associated diminished reddening of dust relative to overall dust emission in those directions) will be difficult.

## 5. Summary

Both Burstein & Heiles (1978b) (the BH method) and Schlegel, Finkbeiner, & Davis (1998) (the IR method) permit one to independently predict line-of-sight Galactic reddening. Both methods can be differentially calibrated using independent reddening estimates for objects situated beyond the Galactic reddening layer. The currently best data for this exercise are the  $(B-V)_0$  colors and  $Mg_2$  line strengths for giant elliptical (gE) galaxies, as it is found empirically (Burstein et al. 1988) that their stellar populations are remarkably uniform for these these parameters. This paper presents a revised 7 Samurai database from which reddening predictions can be made more accurately for 402 gE galaxies. Of these 402 gE galaxies, 12 lack direct BH predictions, one lacks direct IR prediction, and 11 galaxies lie in the southern region identified in Burstein et al. (1987) as needing an adjustment to the BH predictions ( $230^\circ > l > 310^\circ$ ,  $-20^\circ < b < 20^\circ$ ), leaving 378 galaxies for an objective, least-squares analysis.

Both BH and IR methods must assume zero points for their predictions. The BH method uses independent estimates of  $E(B-V)$  at the NGP and takes its zero point

from the directions with the least amount of reddening and minimum amount of average stellar polarization ( $E(B-V) \sim 0.00$ ). The IR method assumes that there is a one-to-one relationship between dust emission/temperature and reddening. Because the IR method sees dust emission at the poles, the BH and IR methods differ in zero point by  $\sim 0.02$  mag. The present analysis is consistent with this finding: IR zero point higher by 0.016 mag when the BH zero point is applied to the IR data, and higher by 0.019 mag when the IR zero point is applied to the BH data.

Two slopes are used for the  $(B-V)_0$ - $Mg_2$  relation, owing to differences in how this relation can be defined. The sample is further divided into low/high reddening directions, as well as taking the whole dataset together (taking the low/high reddening cut at  $E(B-V) = 0.100$ ). For each of these twelve data combinations, a system of four coupled equations in four unknowns are formed that can be solved in a least-squares manner for the intrinsic  $1\sigma$  errors for four quantities of interest: BH-predicted reddenings; IR-predicted reddenings; the agreement between the BH and IR reddening predictions, and the  $(B-V)_0$ - $Mg_2$  relation itself.

In directions with  $E(B-V) < 0.10$  mag, IR prediction errors are 0.002-0.005 mag in  $E(B-V)$  more accurate than those of the BH method, yielding an average  $1\sigma$  prediction accuracy of 0.007 mag. The IR method is more accurate (0.011 mag) than the BH method in most highly-reddened directions (0.024-0.025 mag). Owing to a selection effect first detailed by (Burstein & Heiles 1978a), the higher accuracy of the IR method is likely related to its smaller pixel size on the sky ( $6'$ ) compared to that of the BH method ( $18' \times 36'$ ). Observational errors in the  $(B-V)_0$ - $Mg_2$  relation are 0.027 mag in low reddening directions and higher in high-reddening directions, owing to observational issues in accurately measuring galaxy colors in crowded stellar regions. Only 6 galaxies, all likely companions of larger galaxies, are found in low-reddening directions for which their  $(B-V)$  colors are

significantly too blue or too red for their  $Mg_2$  line strengths. These galaxies are worth further investigations.

Discussion of the reddening at the North Galactic Pole is updated from that given in Burstein & Heiles (1978b), but the same conclusion is drawn from newer data as was drawn then: there are directions around the NGP that have  $E(B-V) \ll 0.01$  mag; i.e, essentially not measurable. Furthermore, a plausible case can be made that the Solar System is presently moving through an old Heiles-type superbubble (Heiles 1979), in which the dust has been affected by the same mechanism (a whittling-down of its ice mantles?; cf. Greenberg & Li (1995)) that produces high gas-to-dust ratios around OB associations (which are seen in both the BH and IR datasets).

IR and BH methods both find large variations in the HI-to-reddening ratio in the interstellar medium in our region of the Galaxy. High ratios of gas-to-dust are found specifically around nearby OB associations and at the Galactic poles. Both methods predict many lines-of-sight where  $E(B-V) < 0.015$  mag, including five gE for which the IR method predicts  $E(B-V) < 0.008$  mag.

There are two lines of evidence that the IR method overpredicts reddenings by  $E(B-V) \sim 0.02$  mag in directions where there are high gas-to-dust ratios: the much larger errors and larger  $E(B-V)$  zero point (0.033 mag) of the IR method relative to the BH method for 11 highly-reddened gE galaxies in directions known to have high gas-to-dust ratios; and the existence of the  $E(B-V) \sim 0.02$  mag zero point difference determined primarily at high Galactic latitudes, which are also directions of high gas-to-dust ratios. Another set of data which could bear on this issue, that of the IR:HI map published in Schlegel et al., seems to be at odds with a similar HI:dust map published in Heiles (1976), and used by BH to correct for gas-to-dust ratio differences in their reddening map. While structure in the IR:HI difference map of Schlegel et al. corresponds well to similar structure in the IR:BH

difference map they publish, the issue as to what the IR:HI map means needs to be resolved before this comparison can be used to help understand zero point difference between the IR and BH methods.

Given the good differential agreement between the BH and IR predictions for most directions where  $E(B-V) < 0.100$  mag, it is wise to compare the reddening estimates one gets from both methods to discover the systematic errors in both methods. In so doing, one can find out further information about what portions of the dust are doing the reddening, as this information is currently unknown. For example, the recent study of Colless et al. (2001) found that taking an average of the two methods yielded a more accurate result than from either method alone.

As long as there was one accurate method for predicting reddening along lines-of-sight (BH) in the Galaxy, the issue of the assuming the zero point of that method was apparently well-hidden from sight. The fact that there are now two accurate methods for predicting line-of-sight reddening in the Galaxy that have assumed different zero points gives us both the chance to learn more about the interstellar medium, but also places the onus of choosing a common zero point upon the user of either or both methods. Inspection of the reddenings from the two methods currently listed on the NED website brings this issue to the forefront. Having two accurate methods of predicting line-of-sight reddenings in our Galaxy gives one the ability to compare them in all directions that are used. Given that systematic differences do exist in these predictions, it is further recommended that the values of the two predictions be compared for consistency before averaging.

In closing, it is hoped that the Sloan Digital Sky Survey (SDSS) will provide a new treasure-trove of E galaxy colors and spectral line strengths which can be used to differentially test the BH and IR reddening predictions in many different directions. Unfortunately, even the SDSS will not probe into highly-reddened, high gas-to-dust regions,

leaving those kinds of investigation for the future. It is also hoped that Schlegel et al. will post files on their website that tabulate both the gas-to-dust ratios that their method calculates and the IR to BH differences with the zero point difference between these data removed. Such tables would facilitate further studies of the the ISM, as well as differences in reddening predictions between the BH and IR methods.

DB would like to thank the NED team, specifically Harold Corwin, Marion Schmitz and Anne Kelly for providing their values for the Schlegel et al. reddenings. An anonymous referee is thanked for helpful comments. DB also thanks his colleagues in the 7 Samurai collaboration for helping to develop one of the most accurate set of data on elliptical galaxies that currently exists.

## REFERENCES

- Appenzeller, I., 1975, *A&A*, 38, 113
- Bender, R., Burstein, D., & Faber, S.M. 1993, *ApJ*, 411, 153
- Berdyugin, A. & Teerikorpi, P., 2002, *A&A* 384, 1050
- Boulanger, F., Abergel, A., Bernard, J.-P., Burton, W.B., Desert, F.-X., Hartmann, D., Lagache, G., & Puget, J.-L., 1996, *A&A*, 312, 256
- Burstein, D., Davies, R.L., Dressler, A., Faber, S.M., Stone, R.P.S., Lynden-Bell, D., Terlevich, R. & Wegner, G. 1987, *ApJS*64, 601
- Burstein, D., Davies, R.L., Dressler, A., Faber, S.M., Lynden-Bell, D., Terlevich, R., & Wegner, G., 1988, *Towards Understanding Galaxies at High Redshift*, ed. R.G. Kron & A. Renzini, (Kluwer, Dordrecht), p. 17
- Burstein, D. & Heiles, C. 1978a, *Ap Lett*, 19, 69
- Burstein, D. & Heiles, C. 1978b, *ApJ*, 225, 40
- Burstein, D. & Heiles, C. 1982, *AJ*, 87, 1162
- Burstein, D. & Heiles, C. 1984, *ApJS*, 54, 33
- Colless, M., Saglia, R.P., Burstein, D., Davies, R.L., McMahan, R.K. Jr., & Wegner, G., 2001, *MNRAS*, 321, 277
- Davies, R.L., Burstein, D., Dressler, A., Faber, S.M., Lynden-Bell, D., Terlevich, R., & Wegner, G. 1987, *ApJS*, 64, 581
- de Vaucouleurs, G., de Vaucouleurs, A., & Corwin, H.G. 1976, *The 2nd Reference Catalogue of Bright Galaxies*, (Univ. of Texas Press, Austin).

- Faber, S.M., Wegner, G., Burstein, D., Davies, R.L., Dressler, A., Lynden-Bell, D., & Terlevich, R., 1989, *ApJS*, 69, 763
- Greenberg, J.M. & Li, A., 1995, in *The Opacity of Spiral Disks*, ed. J.I. Davies & D. Burstein, (Kluwer, The Netherlands), p. 19
- Heiles, C., 1976, *ApJ*, 204, 379
- Heiles, C., 1979, *ApJ*, 229, 533
- Hudson, M., 1999, *PASP*, 111, 57
- Li, A. & Greenberg, J.M., 1997, *A&A*, 323, 566
- Lynden-Bell, D., Faber, S.M., Burstein, D., Davies, R.L., Dressler, A., Terlevich, R., & Wegner, G. 1988, *ApJ*, 326, 19
- Markannen, T., 1979, *A&A*, 74, 201
- Sandage, A., 1973, *ApJ*, 183, 711
- Sandage, A., 1975, *ApJ*, 202, 563
- Schlegel, D. J., Finkbeiner, D. P., & Davis, M. 1998, *ApJ*, 500, 525
- Strittmatter, R.E., Balasubrahmanyam, V.K., Protheroe, R.J., & Ormes, J.F., 1985, *A&A*, 143, 249
- Teerikorpi, P., 1990, *A&A*, 235, 362
- Trager, S.C., Faber, S.M., Worthey, G., & Gonzalez, J.J., 2000, *AJ*, 120, 165
- Tully, R.B., 1988, *Nearby Galaxies Catalog*, Cambridge Univ Press, New York
- VandenBerg, D.A., Bolte, M., & Stetson, P.B. 1990, *AJ*, 100, 445



Table 1. The Reddening Data

Galaxy	Dec	l	b	(B-V)	Mg <sub>2</sub>	BH	BH+	IR	IR-	Dif1	Dif2	Ave(BH+,IR)	Ave(BH,IR-)
N 2012	-79.89	292.02	-30.54	1.10	0.287	0.111	0.130	0.147	0.131	-0.017	-0.020	0.139	0.121
N 6876	-71.02	324.13	-32.60	1.03	0.304	0.040	0.059	0.045	0.029	0.014	0.011	0.052	0.035
N 2434	-69.17	281.00	-21.54	1.09	0.260	0.177	0.196	0.248	0.232	-0.052	-0.055	0.222	0.205
N 3136	-67.13	287.99	-9.45	1.03	0.280	...	...	0.238	0.222	...	...	...	...
N 3136B	-66.73	288.18	-8.81	1.12	0.272	...	...	0.198	0.182	...	...	...	...
N 7192	-64.56	326.52	-44.54	0.95	0.270	-0.003	0.016	0.034	0.018	-0.018	-0.018	0.025	0.009
N 2305	-64.21	274.43	-24.55	1.00	0.304	0.071	0.090	0.076	0.060	0.014	0.011	0.083	0.066
N 6483	-63.67	330.07	-18.66	0.98	0.280	0.077	0.096	0.059	0.043	0.037	0.034	0.078	0.060
N 2887	-63.60	282.27	-9.64	1.12	0.260	...	...	0.225	0.209	...	...	...	...
N 6721	-57.85	338.57	-23.90	1.02	0.338	0.064	0.083	0.060	0.044	0.023	0.020	0.072	0.054

Note. — Column 1 is the name of the galaxy as given in Faber et al. (1989); Column 2 is its 1950 declination (needed to separate the BH subsets into north and south subsets), by which this table is ordered; Columns 3 and 4 are its Galactic longitude and latitude; Column 5 is its *observed* (B-V) color, not corrected for reddening; Column 6 is its revised Mg<sub>2</sub> line-strength, described above; Column 7 is its predicted BH reddening (negative values explicitly given); Column 8 is its predicted BH reddening with 0.019 mag added to bring it into zero point agreement with the IR method; Column 9 is its IR-predicted reddening as given by Schlegel et al.; Column 10 is its IR-predicted reddening with 0.016 mag subtracted, making it consistent in zero point with the BH prediction; Columns 11&12 are its differences in E(B-V), BH+0.019 mag minus IR and BH minus IR-0.016 mag, respectively (see definitions of these terms below); Column 13 averages the BH+0.019 mag and the IR mag predictions for this galaxy; Column 14 averages its BH and its IR-minus-0.016 mag predictions. All predicted negative reddening values, IR or BH, are set to 0.000 for reddening calculations. No values are given in their respective columns when there is either no BH or no IR prediction (these missing values are set to -0.999 in the ASCII version of this table).

13 gE galaxies do not have direct BH or IR reddenings: six gE galaxies have  $b < |10^\circ|$ , where BH predictions do not exist (IC 2311, NGC 2380, NGC 2663, NGC 2887, NGC 3156, and NGC 3156B). Six gE galaxies are in various gaps in the BH reddening map where HI data are absent, hence no direct BH predictions (NGC 641, NGC 822, IC 1459, IC 1625, IC 5328, and ESO 409-G12). NGC 221 (M32) has no direct IR prediction. A further 11 gE galaxies in the region  $230^\circ < l < 310^\circ$ ,  $-20^\circ < b < 20^\circ$  were found in Lynden-Bell et al. (1988) and Burstein et al. (1987) to have HI-only BH reddening predictions that are a factor of two too high (NGC 2292, NGC 2293, NGC 2325, NGC 2888, NGC 2904, NGC 3087, NGC 3250, NGC 3557, NGC 4976, ESO 208-G21, and ESO 264-G31). (These galaxies are noted in this table by an asterisk in their names.) Note that an additional 11 galaxies within a smaller region defined by  $265^\circ < l < 310^\circ$ ,  $17^\circ < b < 19.5^\circ$  (NGC 3108, NGC 3258, NGC 3257, NGC 3260, E376-G007, E318-G021, NGC 4946, NGC 5011, NGC 5090 and E270-G014) did *not* need to have their reddenings so-corrected in the 7 Samurai database.

Table 2. Least-Squares-Determined Observational and Intrinsic Errors.

Data Set	N	BH:BV	IR:BV	Ave:BV	BH:IR	$\sigma(\text{BH})$	$\sigma(\text{IR})$	$\sigma(\text{Ave})$	$\sigma(\text{BV} + \text{Mg}_2)$
All:1.12:BH+	378	306	293	288	158	128	93	79	278
		22	31	21	16				
Low:1.12:BH+	344	295	288	282	144	112	91	71	273
		24	28	21	12				
High:1.12:BH+	34	399	340	347	263	237	114	132	321
		7	52	25	52				
All:1.12:IR-	378	309	292	292	144	125	72	72	283
		16	22	14	-6				
Low:1.12:IR-	351	298	286	285	129	110	69	65	277
		17	19	13	-10				
High:1.12:IR-	27	427	361	372	266	248	98	133	348
		3	59	26	43				
All:0.942:BH+	378	297	282	279	158	130	91	79	267
		0	18	-1	16				
Low:0.942:BH+	344	287	277	273	144	114	87	72	263
		1	15	-2	12				
High:0.942:BH+	34	386	325	332	263	237	114	132	304
		-10	44	6	52				
All:0.942:IR-	378	301	281	282	144	127	68	72	273
		-6	16	10	-10				
Low:0.942:IR-	351	291	275	276	129	113	63	65	268
		-6	16	10	-10				
High:0.942:IR-	27	408	345	354	266	244	107	133	327
		-15	60	28	43				

Note. — Column 1 gives the type of sample used (BH+ or IR- refers to the addition/subtraction of zero points for that data set, 1.12/0.942 refers to the slope of the  $(\text{B}-\text{V})_0\text{-Mg}_2$  relation used, all/low/high refers to the subset of data used). Column 2 gives the number of galaxies in this sample. Columns 3-6 give the  $1\sigma$  least-squares errors in  $E(\text{B}-\text{V})$  found for the observable errors (BH:BV, IR:BV, Ave:BV, and BH:IR, respectively), in units of 0.0001 mag. Columns 7-10 give the  $1\sigma$  least-squares errors derived from the least-squares solution of the above equations for the intrinsic errors  $\sigma(\text{BH})$ ,  $\sigma(\text{IR})$ ,  $\sigma(\text{Ave})$  and  $\sigma(\text{BV} + \text{Mg}_2)$ , in units of 0.0001 mag. The second line in this table gives the zero point offsets calculated for each of the least-squares fits under which they are placed.

Table 3. Galaxies Separately Disussed

Galaxy	l	b	E(B-V) <sub>BH</sub>	E(B-V) <sub>IR-</sub>	E(B-V) <sub>BH+</sub>	E(B-V) <sub>IR</sub>	Diff <sub>BH:IR</sub>	Diff <sub>BH</sub>	Diff <sub>IR</sub>	Diff <sub>gal</sub>
Four galaxies for which IR reddenings more accurate than BH reddenings										
NGC 1060	148.77	-24.79	0.117	0.193	0.136	0.209	-0.075	0.078	0.003	0.040
NGC 1293	150.94	-13.16	0.208	0.151	0.227	0.167	0.059	-0.115	-0.057	-0.087
NGC 1713	198.62	-24.50	0.062	0.108	0.081	0.124	-0.045	0.061	0.017	0.039
NGC 5017	310.32	45.80	0.024	0.068	0.043	0.084	0.043	0.053	0.010	0.031
Four galaxies for which BH reddenings more accurate than IR reddenings										
NGC 821	151.55	-47.56	0.040	0.094	0.059	0.110	-0.053	-0.020	-0.071	-0.046
E208*G021	262.69	-14.30	0.075	0.157	0.094	0.173	-0.081	0.015	-0.066	-0.027
NGC 2434	281.00	-21.54	0.177	0.232	0.196	0.248	-0.054	0.001	-0.053	-0.027
NGC*4976	305.80	13.27	0.112	0.167	0.131	0.183	-0.054	-0.027	-0.080	-0.054
One galaxy for which BH and IR reddenings differ but both accurate										
NGC*2888	257.15	16.08	0.057	0.108	0.076	0.124	-0.050	0.014	-0.037	-0.012
Six galaxies for which BH and IR reddenings agree, but galaxy (B-V) <sub>0</sub> deviates										
NGC 83	113.86	-39.91	0.032	0.054	0.051	0.070	-0.021	0.091	0.070	0.080
NGC 708	136.58	-25.08	0.060	0.072	0.079	0.088	-0.011	0.105	0.094	0.099
NGC 1549	265.41	-43.80	0.000	0.000	0.000	0.013	-0.007	-0.069	-0.076	-0.073
NGC 3610	143.54	54.46	0.000	0.000	0.013	0.010	-0.002	-0.089	-0.086	-0.088
NGC 4872	57.85	88.02	0.012	0.000	0.031	0.009	0.017	0.082	0.098	0.090
NGC 7617	87.64	-48.35	0.040	0.069	0.059	0.085	-0.028	0.141	0.114	0.128
The Seven Other Perseus Galaxies (in addition to NGC 1293)										
IC 310	150.18	-13.73	0.149	0.144	0.168	0.160	0.007	0.054	0.060	0.056
NGC 1272	150.51	-13.33	0.162	0.146	0.181	0.162	0.018	-0.031	-0.012	-0.022
NGC 1273	150.50	-13.28	0.174	0.147	0.193	0.163	0.029	-0.033	-0.004	-0.019
NGC 1278	150.56	-13.21	0.174	0.148	0.193	0.164	0.028	-0.021	0.007	-0.007
NGC 1282	150.72	-13.34	0.171	0.151	0.190	0.167	0.022	-0.058	-0.036	-0.047
NGC 1283	150.71	-13.31	0.171	0.150	0.190	0.166	0.023	-0.023	0.001	-0.012
CR 32	150.51	-13.22	0.174	0.149	0.193	0.165	0.027	0.017	0.044	0.030
The Additional Eight High Gas-to-Dust Galaxies in the $230^\circ > l > 310^\circ$ , $-20^\circ < b < 20^\circ$ Direction										
N*2292	236.73	-12.61	0.141	0.103	0.160	0.119	0.040	-0.018	0.022	0.002
N*2293	236.74	-12.60	0.141	0.104	0.160	0.120	0.039	-0.031	0.008	-0.011
N*2325	239.96	-10.41	0.140	0.101	0.159	0.117	0.041	-0.016	0.025	0.005
N*2904	259.52	15.06	0.083	0.110	0.102	0.126	-0.026	0.006	-0.021	-0.008
N*3087	266.89	16.33	0.072	0.090	0.091	0.106	-0.017	0.011	-0.007	0.002
N*3250	274.97	14.93	0.066	0.087	0.085	0.103	-0.020	0.011	-0.009	0.001

Table 3—Continued

Galaxy	l	b	$E(B-V)_{\text{BH}}$	$E(B-V)_{\text{IR-}}$	$E(B-V)_{\text{BH+}}$	$E(B-V)_{\text{IR}}$	$\text{Diff}_{\text{BH,IR}}$	$\text{Diff}_{\text{BH}}$	$\text{Diff}_{\text{IR}}$	$\text{Diff}_{\text{gal}}$
N*3557	281.58	21.09	0.069	0.083	0.088	0.099	-0.013	0.033	0.020	0.026
E264*G031	280.53	10.91	0.100	0.139	0.119	0.155	-0.038	0.043	0.005	0.024

Note. — Column 1 gives the galaxy name; Columns 2 and 3 give the Galactic longitude and latitude of this galaxy; Columns 4-7 give, respectively, the BH reddening, the IR-0.016 reddening, the BH+0.019 reddening and the IR reddening predicted for this galaxy; Column 8 gives the difference, BH-IR, taking the average of the differences BH minus IR-0.016 and BH+0.019 minus IR; Columns 9-11 give, respectively, the difference in  $(B-V)_0$  for this galaxy from the  $(B-V)_0$ - $\text{Mg}_2$  relationship using: a) the average of the two BH predictions (BH, BH+0.019); b) the average of the two IR predictions (IR, IR-0.016), and c) the average difference overall by combining all four predictions.

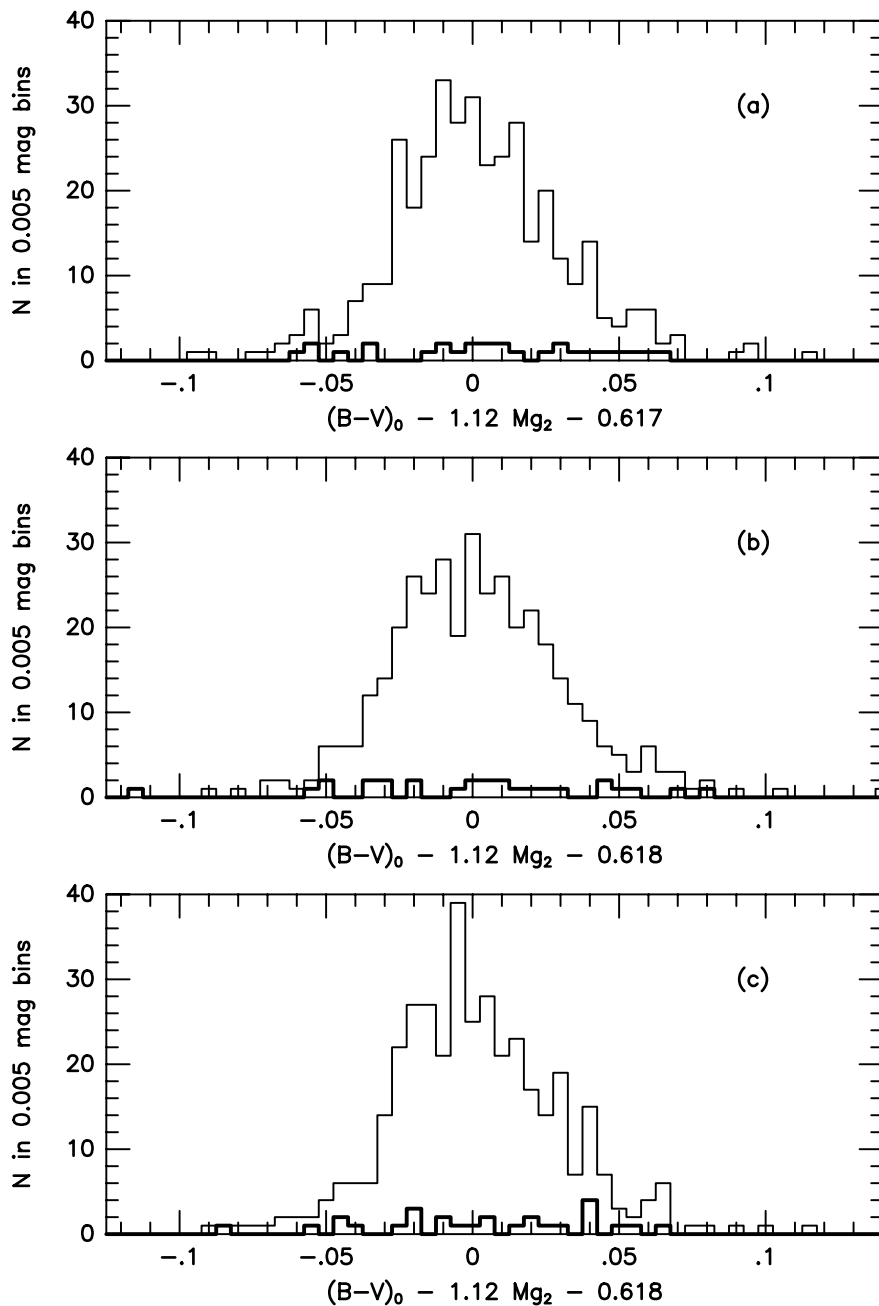


Fig. 1.— The histograms of residuals from the  $(B-V)_0$ - $Mg_2$  relation for the 378 galaxy sample using the 1.12 slope for this relation. The histograms for the highly-reddened galaxies are given in darker lines: (a) the IR-0.016 predictions; (b) for the straight BH predictions; (c) for the average of IR-0.016 and BH predictions.

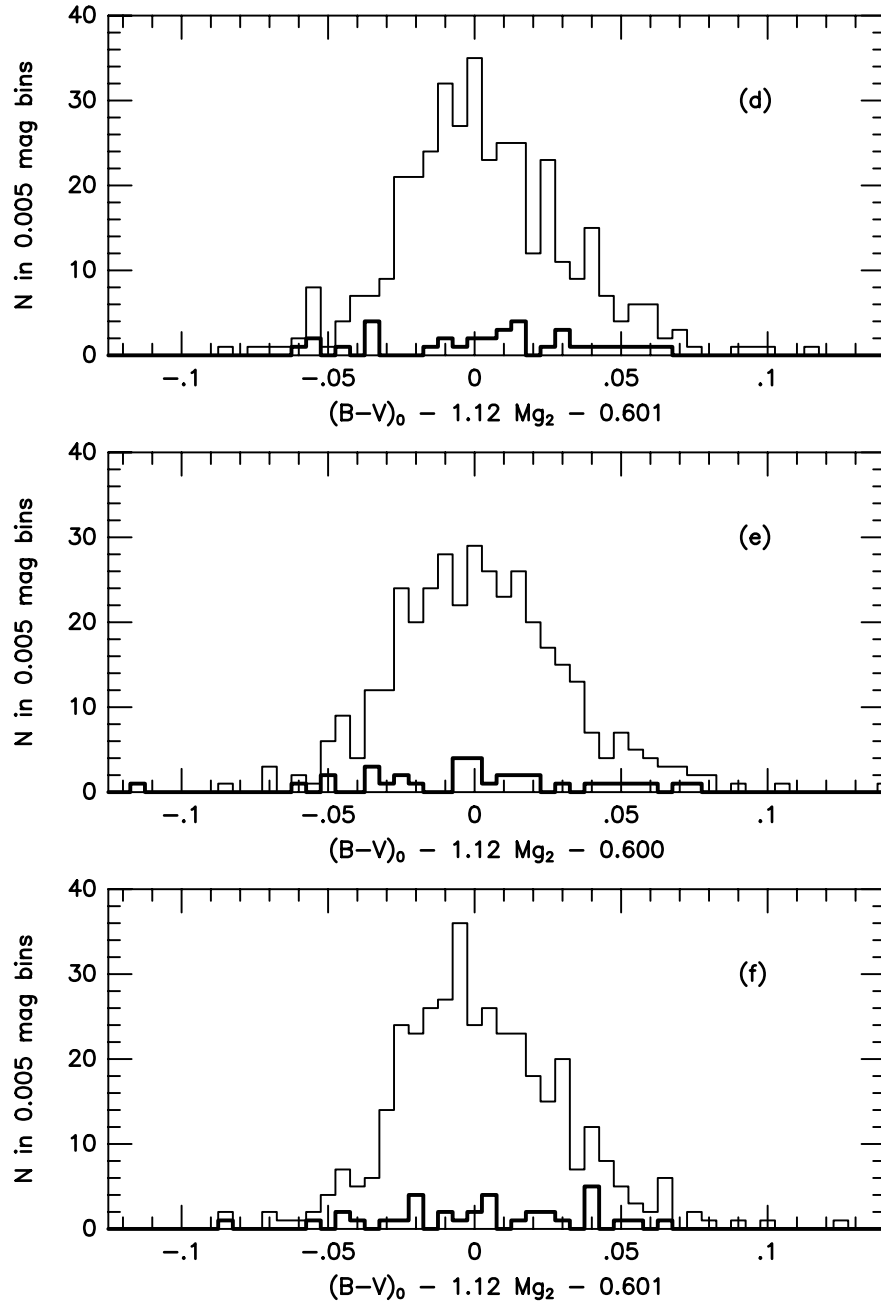


Fig. 1.— (continued): (d) for the straight IR predictions; (e) for the BH+0.019 predictions; and (f) the average of IR and BH+0.019 predictions.

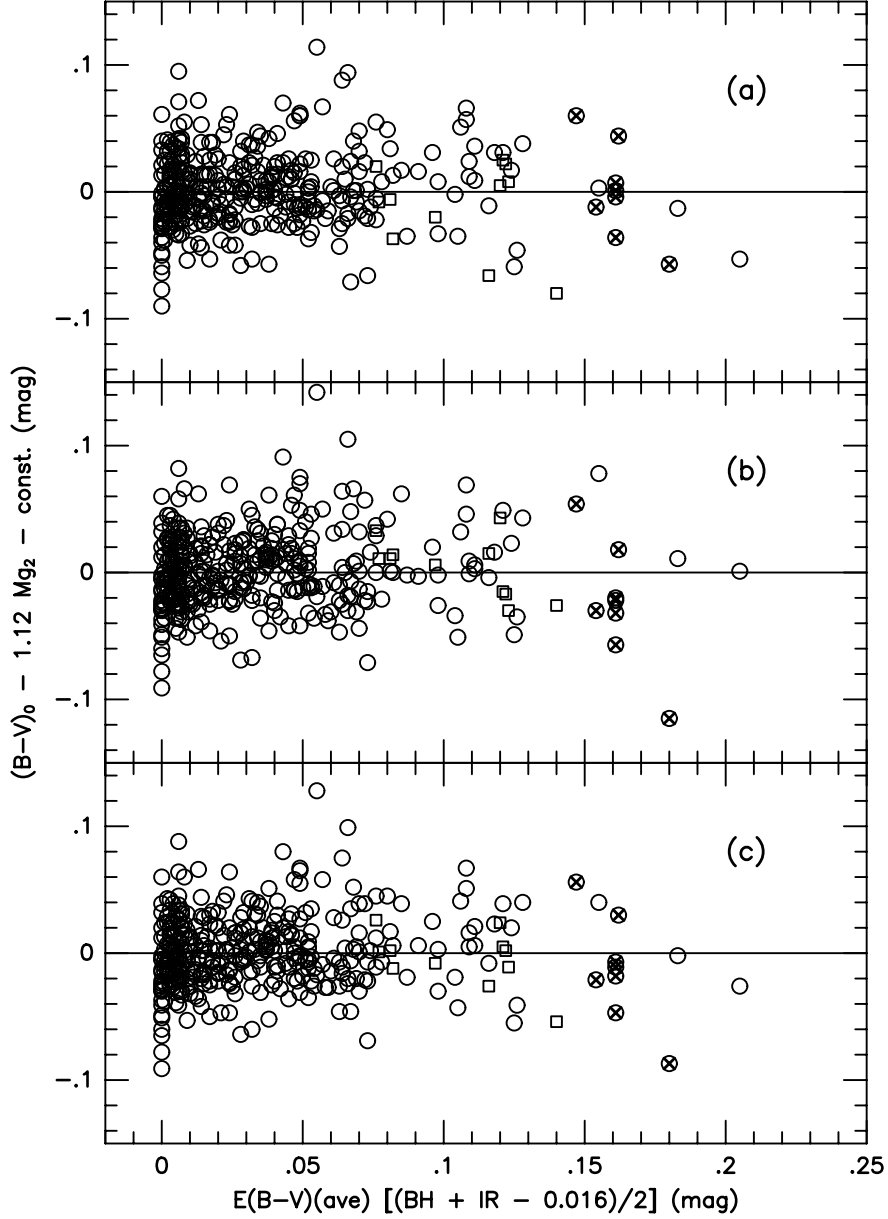


Fig. 2.— The residuals from the  $(B-V)_0$ - $\text{Mg}_2$  relation plotted versus the Ave value of  $E(B-V)$  for each galaxy: (a) the IR-0.016 predictions; (b) for the BH predictions; (c) for the average of IR-0.016 and BH predictions. Data for galaxies in the Perseus cluster are plotted as circled X's; data for the 11 highly-reddened galaxies in the region  $230^\circ > l > 310^\circ$ ,  $-20^\circ < b < 20^\circ$  are added to this figure and are plotted as open boxes in each graph.

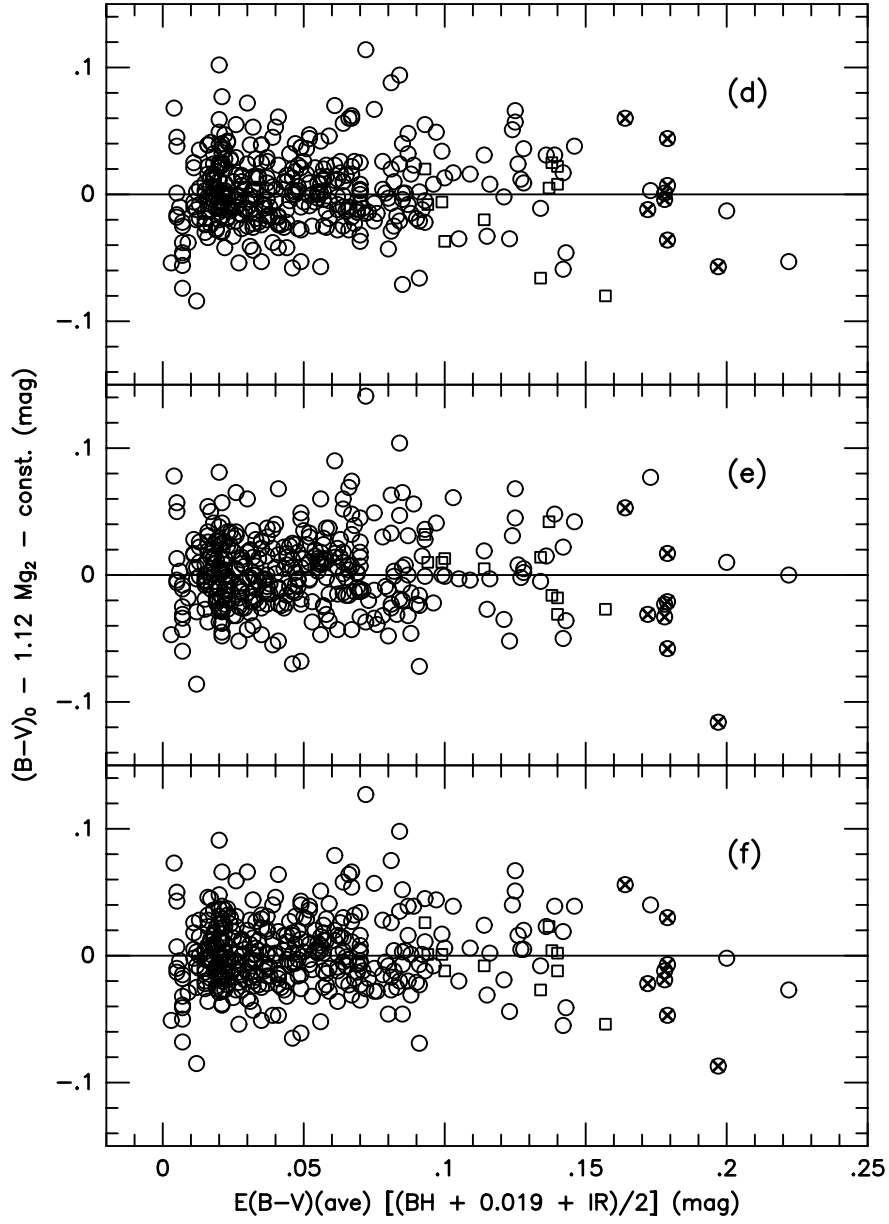


Fig. 2.— (continued): (d) for the straight IR predictions; (e) the BH+0.019 mag predictions; and (f) the average of BH+0.019 and IR predictions.

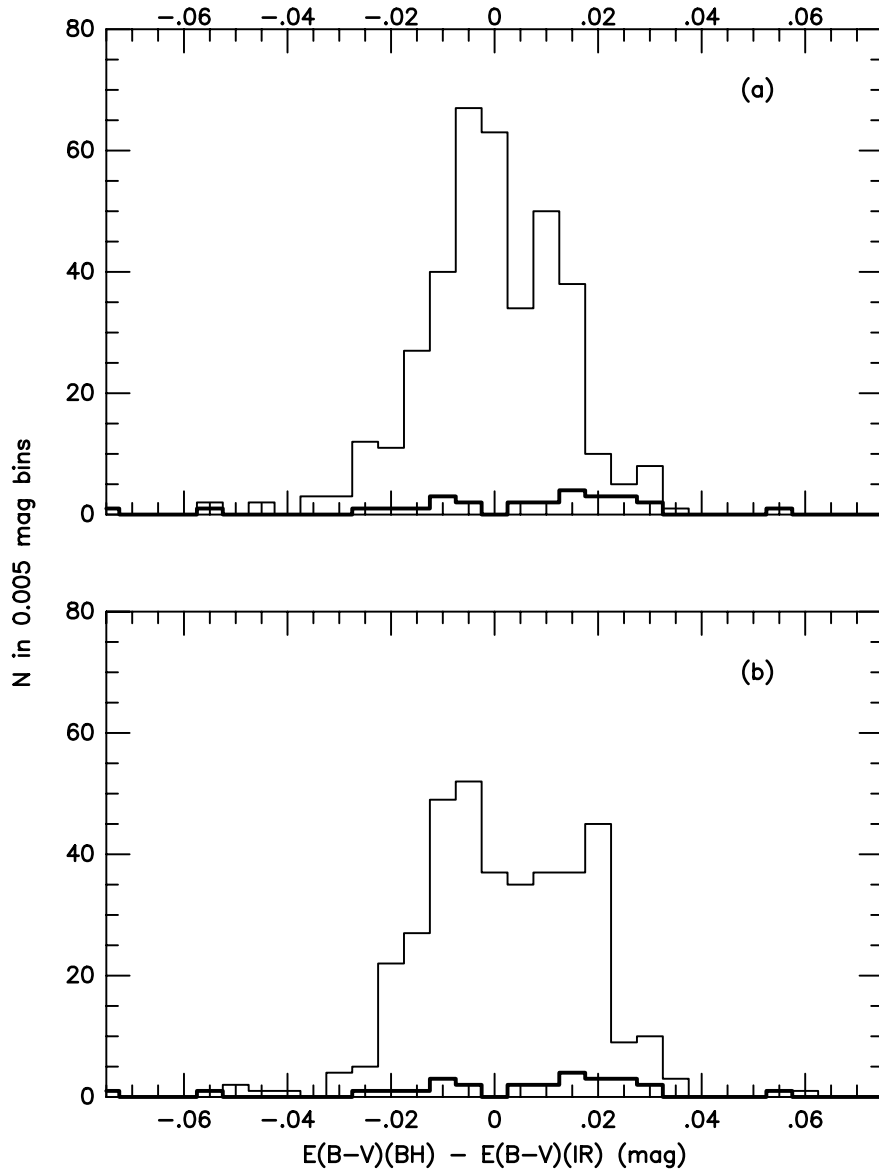


Fig. 3.— The histograms of  $E(B-V)$  prediction differences, in the sense BH minus IR, for (a) the BH minus IR-0.016 predictions; and (b) for the BH+0.019 minus IR predictions. As with Figure 1, the histograms for the highly-reddened galaxies are given as a dark line.

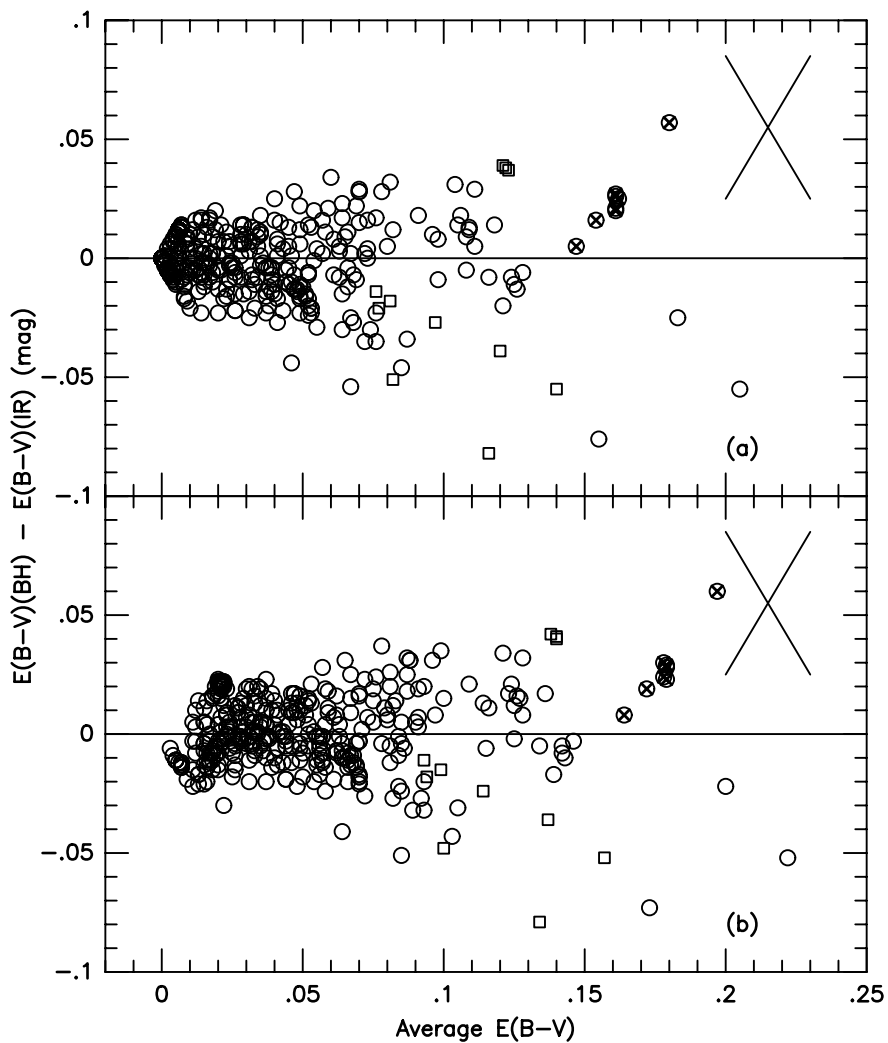


Fig. 4.— Graphs of the difference, BH minus IR predictions for reddening versus the average reddening for the two predictions: a) BH, IR-0.016 values; b) BH+0.019, IR values. If the difference between the two reddening predictions is systematic, then they should follow the lines plotted in each graph. The symbols for the galaxies in the Perseus cluster and in the high gas-to-dust region in the southern hemisphere region are as in Figure 2.

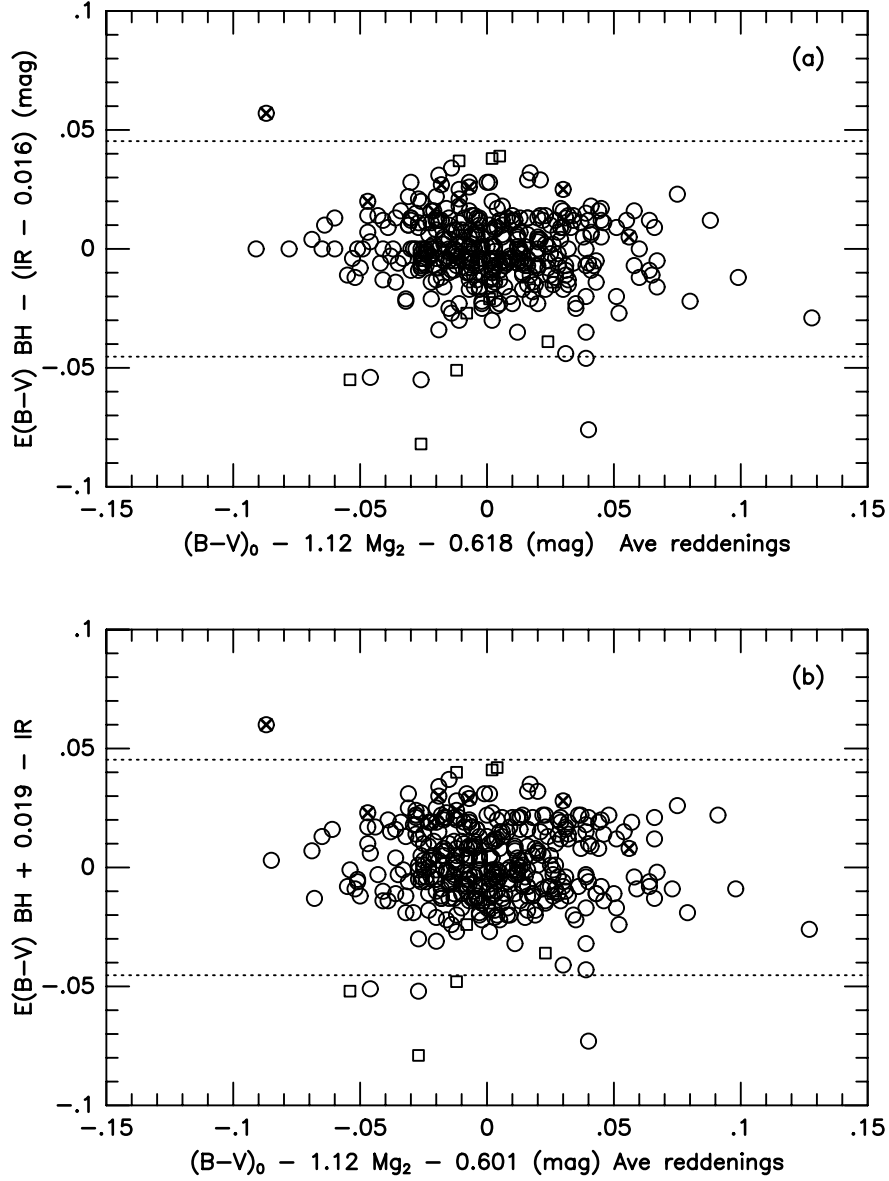


Fig. 5.— Graphs of the difference, BH minus IR predictions for reddening versus the scatter in the  $(B-V)_0$ - $Mg_2$  relation using the average reddenings: a) BH, IR-0.016 values; b) BH+0.019, IR values. The symbols for the galaxies in the Perseus cluster and in the high gas-to-dust, southern hemisphere region are as in Figure 2.